[9]T. M. Rice and D. B. McWhan, IBM J. Res. Develop. 14, 251 (1970).

[10]J. B. Goodenough, in *Progress in Solid State Chemistry*, edited by H. Reiss (Pergamon, Oxford, 1971), Vol. 5, pp. 145ff.

[11]R. W. Vest and J. M. Honig, in *Electrical Conductivity of Ceramics*, edited by N. M. Tallan (Marcel Dekker, New York, to be published).

[12]C. S. Fadley, Lawrence Radiation Laboratory Report No. UCRL-19535, 1970 (unpublished).

[13]J. A. Bearden and A. F. Burr, Rev. Mod. Phys. 39, 125 (1967).

[14]D. W. Fischer, J. Appl. Phys. 40, 4151 (1969); 41, 3561 (1970).

[15]R. J. Powell, Stanford Electronics Laboratory Technical Report No. 5220-1, 1967 (unpublished).

[16]W. M. H. Sachtler, G. J. H. Dorgelo, and A. A. Holscher, Surface Sci. 5, 221 (1966).

[17]W. L. Jolly and D. N. Hendrickson, J. Am. Chem. Soc. 92, 1863 (1970).

[18]I. Nebenzahl and M. Weger, Phil. Mag. 24, 1119 (1971).

PHYSICAL REVIEW B VOLUME 6, NUMBER 4 15 AUGUST 1972

Photoelectronic Properties of Zinc Impurity in Silicon†

Alden F. Sklensky*

Department of Materials Science, Stanford University, Stanford, California 94305
and Lockheed Palo Alto Research Laboratories, Palo Alto, California 94304

and

Richard H. Bube

Department of Materials Science, Stanford University, Stanford, California 94305

(Received 23 February 1972)

Zinc impurity in high-resistivity n-type-silicon single crystals exhibits the properties of a sensitizing center for photoconductivity; the electron lifetime is increased by a factor of 10^4 to a value of 100 msec at 80 °K. A variety of photoelectronic measurements are used to determine the location of the Zn^{-2} energy level with respect to the conduction- and valence-band edges, the density of zinc centers, the change in scattering cross section upon photoexcitation, the electron-capture cross section of the Zn^{-1} center as a function of temperature, and the existence and properties of other imperfection states. Optical quenching of photoconductivity indicates an electron-capture cross section of the Zn^{-1} center which is about 10^{-20} cm^2 and independent of temperature below 50 °K, and which decreases exponentially with $1/T$ at higher temperatures with an activation energy of 40 meV. Measurements of temperature dependence of steady-state lifetime and of photoconductivity decay time are consistent.

INTRODUCTION

The photosensitivity of infrared detectors using II-VI or III-V compounds[1–6] is frequently enhanced several orders of magnitude by the presence of imperfections which behave as sensitizing centers and increase the free-electron lifetime. Sensitizing centers in II-VI and III-V compounds are generally assumed to be associated with intrinsic defects, but similar sensitizing imperfections associated with specific impurities are known in Ge and Si.[7–21] One of the most interesting of these is the case of Zn impurity in Si,[17–21] which provides an opportunity to investigate the properties of a known sensitizing center in a well-characterized material.

The saturation zinc concentration in silicon as a function of temperature and diffusivity has been established by Fuller and Morin[22] with some later refinements.[23–25] Fuller and Morin, and Carlson[26] report the existence of two acceptor levels associated with Zn as a double acceptor in Si; the possibility of a third acceptor level has been considered by other workers,[23] but its presence does not seem likely.[27,28] Values for the various cross sections associated with these two levels taken from the literature are summarized in Table I.

It was the purpose of the present investigation to explore the properties of Zn impurity in high-resistivity n-type-Si single crystals by the use of a variety of photoelectronic techniques. Of particular interest were the location of the Zn^{-2} energy level, the density of incorporated Zn centers, the scattering cross section associated with Zn impurity, the temperature dependence of the electron-capture cross section of the Zn^{-1} center, and the effects of other imperfections in the Si. The first four properties represent a rather complete characterization of the zinc sensitizing center in silicon and the temperature dependence of S_1^n provides information on the capture process of a Coulombically repulsive center.

TABLE I. Previously reported values for cross sections of zinc impurity in silicon.

Process	Values (cm^2)	Ref.
Electron capture by Zn^0	$5\times10^{-16} < S_0^n < 10^{-15}$	29,30
Hole capture by Zn^{-1}	$10^{-14} < S_1^p < 10^{-13}$	29–31
Electron capture by Zn^{-1}	$10^{-20} < S_1^n < 10^{-16}$	19,32,33
Hole Capture by Zn^{-2}	$10^{-16} < S_2^p < 10^{-13}$	20,32
Optical excitation from valence band to Zn^0	$10^{-16} < S_{opt}^{0v} < 2\times10^{-16}$	34,35
Optical excitation from Zn^{-1} to conduction band	$S_{opt}^{1c} \approx 3\times10^{-15}$	34
Optical excitation from Zn^{-2} to conduction band	$10^{-17} < S_{opt}^{2c} < 10^{-15}$	34,36
Optical excitation from valence band to Zn^{-1}	$S_{opt}^{1v} \approx 2\times10^{-15}$	34

EXPERIMENTAL

Materials

Zinc (99.9998% pure from Cominco American, Inc.) was diffused from a high-pressure (about 2 atm) vapor at 973 °C into float-zone-refined silicon (Wacker Chemie) with 2×10^{15}-cm^{-3} phosphorus-donor impurities and presumably no more than 10^{12}-cm^{-3} total of other impurities. The diffusion process was carried out in an evacuated sealed ampoule with sufficient zinc included to assure zinc vapor would be in equilibrium with zinc liquid at the diffusion temperature. During each diffusion (about 16-h duration) the temperature profile along the ampoule, as well as the temperature as a function of time, was constant to within 0.5 °C. When the diffusion was completed, the ampoule was quenched to room temperature. After diffusion, samples were mechanically polished, then etched, to remove surface erosion and inversion layers. Dimensions of the final Hall samples were about 3.5×1.5×0.1 mm excluding contact arms.

Contacts

Samples were mechanically polished, cleaned, masked, and placed into a vacuum chamber. After 0.5 μm of Au: (0.6 wt.% Sb) was evaporated onto the sample, it was removed from the vacuum chamber and heated in an atmosphere of flowing-forming gas (5% H_2, 95% N_2). Successfully alloyed contacts formed at about 425 °C. The current-carrying contacts of the sample measured in detail were Ohmic.

Measurements

Standard photoelectronic techniques were used in all measurements. The sample was mounted in a Collins hydrogen cryotip, allowing temperature variation between 30 and 300 °K. Monochromatic excitation was obtained with a Bausch and Lomb monochromator with tungsten source; intensity variations were achieved with neutral-density filters.

RESULTS

Temperature Dependence of Equilibrium Hall Coefficient

The Zn-diffused samples were of high resistivity with an electron density of 4×10^{11} cm^{-3} at 300 °K. The temperature dependence of the Hall coefficient[37] was measured between 220 and 300 °K in the dark. If $\ln(RT^{3/2})^{-1}$ is plotted as a function of $1/T$, an activation energy of 0.51 eV is obtained. If the distance of the Fermi level below the conduction band, E_F, is calculated from these data from $n=N_c e^{-E_F/kT}$, it is found that $E_F=(0.51-3.5\times10^{-4}T)$ eV.

Spectral Response of Photoconductivity

An optical value for the ionization energy of an electron from a Zn^{-2} center can be obtained from the low-energy threshold for extrinsic photoconductivity, for comparison with the thermal value for the same quantity obtained from the temperature dependence of equilibrium Hall coefficient. The photoconductivity spectrum measured at 80 °K is given in Fig. 1. If the low-energy portion of the spectrum is plotted as the square root of photoconductivity vs photon energy to obtain a linear relationship, a threshold energy of 0.52 eV is obtained, in good agreement with the thermal-ionization energy.

Optical Quenching Spectrum

A third measure of the location of the Zn^{-2} level can be obtained by determining the low-energy

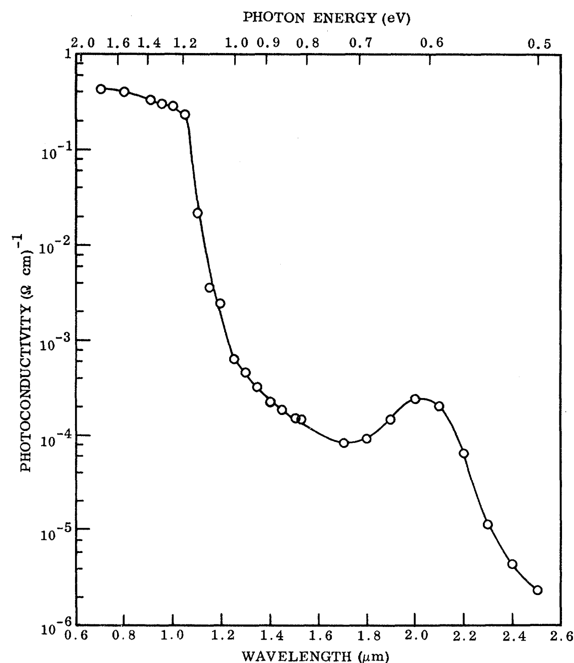

FIG. 1. Photoconductivity spectrum at 80 °K.

threshold for optical quenching of photoconductivity, corresponding to a transition from the valence band to the Zn^{-1} center. The resulting optical-quenching spectra, measured at 80 °K for three different intensities of the quenching radiation and the same primary excitation intensity, are shown in Fig. 2. The low-energy threshold is found to be 0.58 eV. A competition between optical quenching and excitation by the same photons causes the minimum of photoconductivity seen in Fig. 1 in the vicinity of 1.7 μm (0.73 eV). Note that the sum of 0.58 eV, the energy from the valence band to the Zn^{-2} energy level, and 0.51 eV, the energy from the Zn^{-2} energy level to the conduction band, is 1.09 eV, 0.07 eV less than the band gap at 80 °K. Also, 0.58 eV is 0.11 eV less than has been previously reported for the energy difference between the valence band and the Zn^{-2} level. This is discussed in more detail later.

Intensity Dependence at Low Temperatures

Variation of the intensity of photoexcitation at low temperatures would be expected to yield two results characteristic of sensitizing centers: (a) Changing the charge of the Zn impurities from − 2 to − 1 as the result of hole capture would be expected to yield an increased electron mobility; and (b) if sufficiently high intensities were used to empty all the Zn^{-2} centers, a saturation of photoconductivity would be expected, from which

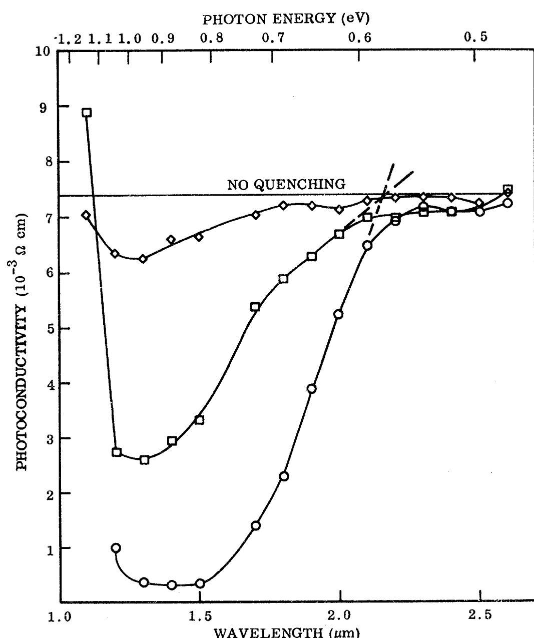

FIG. 2. Quenching spectra at 80 °K for quenching intensities of 2.7×10^{14} (○), 3.8×10^{13} (□), and 4.3×10^{12} (◇) cm^{-2} sec^{-1}. Similar curves have been obtained for quenching of extrinsic photoexcitation.

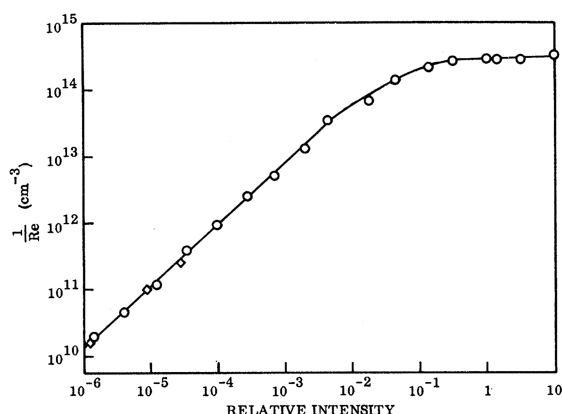

FIG. 3. Carrier density variation with excitation intensity at 80 °K: (○) 0.9-, (◇) 2.3-μm excitation.

the density of Zn centers could be estimated.[38]

The variation of electron density with excitation intensity at 80 °K is shown in Fig. 3, and the corresponding variation of electron mobility in Fig. 4. For low excitation intensities, the electron density is a linear function of intensity (constant-electron lifetime), and for very high intensities, it saturates at a value of 3×10^{14} cm^{-3}. Figure 4 shows that the electron mobility does increase with excitation from a value of about 4200 cm^2/V sec for low intensities to a value of about 7000 cm^2/V sec at high intensities.

Determination of Electron-Capture Cross Section

The value of the electron density at which optical quenching of photoconductivity starts can be used to determine the value of the electron-capture cross section of the Zn^{-1} center.[39] The critical value of electron density can be obtained either by fixing the primary intensity and varying the quenching intensity, or by fixing the quenching intensity and varying the primary intensity. Then the electron cross section is given by

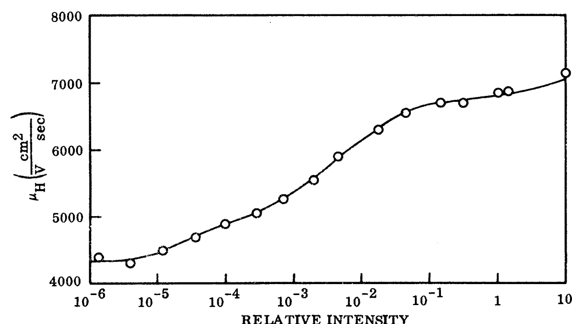

FIG. 4. Mobility variation with intensity of 0.9-μm radiation at 80 °K.

$$S_1^n = f' S_{opt}^{lv} / n^* v \quad , \tag{1}$$

where f' is the quenching-photon flux $cm^{-2}\,sec^{-1}$, n^* is the critical electron density at the onset of quenching, and v is the electron thermal velocity. Values of the electron cross section obtained for different conditions are summarized in Table II, where the value of S_{opt}^{lv} given in Table I has been assumed valid. These values of S_1^n are plotted as a function of temperature in Fig. 5. It appears that S_1^n is approximately independent of temperature at a value of 10^{-20} cm^2 below 80 °K, and that above 80 °K it increases with an activation energy corresponding to 40 meV up to 200 °K.

Temperature Dependence of Photoconductivity

From a knowledge of the temperature dependence of the capture cross section, the temperature dependence of the electron lifetime can be predicted. Two other methods are available for the determination of electron lifetime temperature dependence: (a) steady-state photoconductivity as a function of temperature, and (b) decay time of photoconductivity as a function of temperature as long as trapping effects do not interfere.

The variaton of photoexcited electron density with temperature is shown in Fig. 6 for four different excitation conditions. Similar data from Loebner[17] are included for comparison. For the highest excitation intensity the photoconductivity is saturated and therefore temperature invariant at low temperatures. The minimum in the electron density seen also in the similar curve from Loebner is apparently associated with recombination through other imperfections in the crystal.

TABLE II. Summary of values of electron cross section of Zn^{-1} center (assuming $S_{opt}^{1v} = 2\times10^{-15}$ cm^2).

T (°K)	S_1^n(× 10^{-20} cm^2)	Primary excitation (μm)
31[a]	0.9	0.9[b]
80	0.92–1.3	0.9
	1.5–2.0	2.3[c]
118	1.5	0.9
142	2.4	2.3
140	3.6	0.9
165	8.3	0.9
186	4.8–6.5	0.9
210	9.5	0.9

[a]The measurement at 31 °K is less certain than the others since (i) it is the only measurement made at that temperature, and (ii) no Hall data are available for conversion of the conductivity measurement to a value of n. n was estimated by comparison with the conductivity at saturation intensities, assuming n_{sat} to be independent of temperature.

[b]Intrinsic excitation.

[c]Extrinsic excitation.

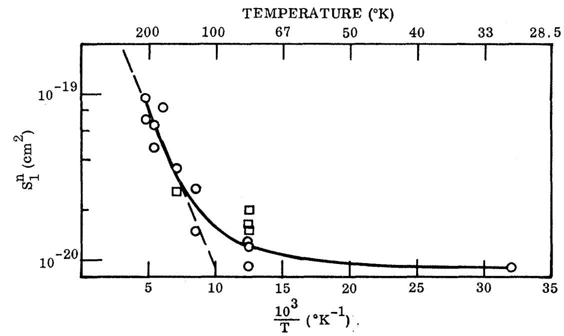

FIG. 5. Variation with temperature of electron-capture cross section of singly negative zinc center (S_1^n). Measurements made by quenching technique with both (○) 0.9- and (□) 2.3-μm exciting radiation. Slope of dashed line gives an activation energy of 40 meV.

The electron lifetime, calculated from a linear portion of the electron density vs excitation intensity dependence, is shown as τ_n as a function of temperature in Fig. 7.

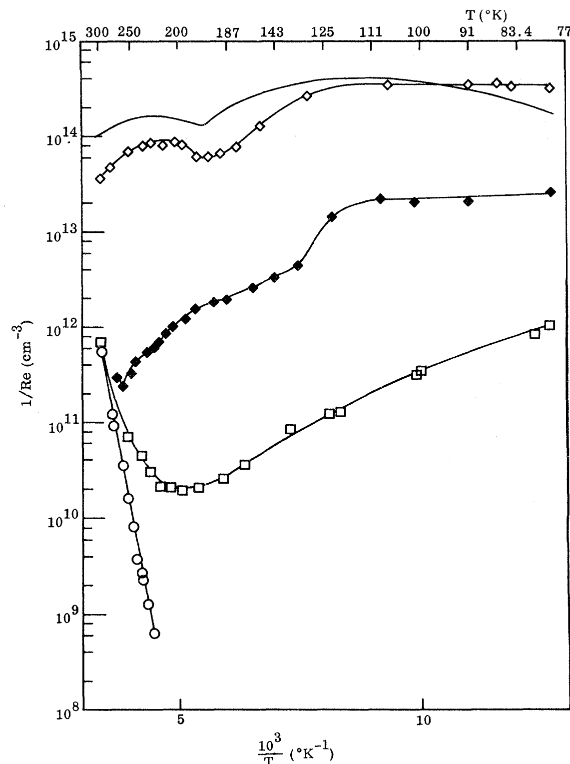

FIG. 6. Variation of carrier density with temperature with (○) no irradiation of the sample, (◇) with irradiation by 0.9-μ light of intensities 3.4×10^{15}, (◆) 6.8×10^{12} $cm^{-2}\,sec^{-1}$, and (□) with irradiation by 2.0-μm light of intensity 7.6×10^{15} $cm^{-2}\,sec^{-1}$. The curve with no data points associated is included for comparison and is from Loebner *et al.* (Ref. 17).

Decay of Photoconductivity

The decay of photoconductivity was measured after establishing a steady-state photoconductivity with low-intensity intrinsic radiation, appropriate to produce an electron density in the linear portion of the electron density vs excitation intensity dependence. Decay curves showed a linear relationship between $\ln n$ and t for all temperatures below 179 °K; above 179 °K this linear relationship was not found and there was evidence that the decay time was being controlled by trap emptying rather than recombination. The time for the conductivity to decay to $1/e$ of its initial value is plotted as a function of temperature in Fig. 7 over the whole measured temperature range, and is indicated as τ_d.

Also shown for comparison in Fig. 7 is the temperature dependence of

$$\tau_{n0} = 1/N_{\mathrm{Zn}} S_1^n v \qquad (2)$$

for a density of zinc centers $N_{\mathrm{Zn}} = 10^{15}$ cm^{-3}, and the values for the cross section S_1^n in Table II, measured by the quenching technique. τ_{n0} is the shortest lifetime obtainable for recombination through the upper zinc level, occurring when all the zinc centers are singly charged.

Thermally Stimulated Conductivity

The variation of τ_d with temperature shown in Fig. 7 indicates the presence of at least one set of trapping levels, which empty above 180 °K.

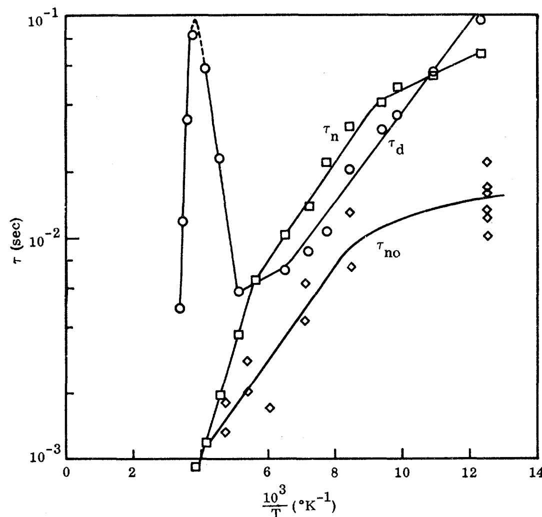

FIG. 7. Variation with temperature of lifetime (□) from steady-state measurements, decay time (○), and τ_{no} (◇), calculated from Eq. (2) using S_1^n values from Fig. 5, and $N_{\mathrm{Zn}} = 10^{15}$ cm^{-3}. Each measurement of steady-state lifetime was measured nearly simultaneously with the corresponding value of decay time in the same experiment.

Another measure of these trapping levels can be obtained from the measurement of thermally stimulated conductivity (TSC), as shown in Fig. 8, after either intrinsic or extrinsic excitation at low temperatures.

Below 150 °K the conductivity is below the measurable limit, while above 150 °K only one set of trapping levels is indicated, corresponding to a TSC maximum at 185 °K. If it is assumed that strong retrapping is involved, the trap depth can be estimated by calculating the location of the Fermi level at the maximum; the value obtained in this way is $E_t = 0.41$ eV. The density of the traps may be estimated from the total charge flowing in the TSC measurement, taking account of the effective gain; a density of 10^{15} cm^{-3} is estimated in this way. Diesel *et al.*[40] reported three trap levels in their material with TSC maxima at 113, 169, and 213 °K, and densities of 6×10^{15}, 2×10^{15}, and 8×10^{14} cm^{-3}, respectively.

DISCUSSION

Location of Zn^{-2} Energy Level

The thermal-ionization energy derived from the temperature dependence of the Hall coefficient (0.51 eV) agrees well with the optical-ionization energy derived from the low-energy threshold for extrinsic photoconductivity (0.52 eV). This energy difference between the conduction band and the Zn^{-2} level, plus the energy difference between the valence band and the Zn^{-1} energy level (see Fig. 9) obtained from the low-energy threshold of the optical-quenching spectrum (0.58 eV) should be equal to the band gap of silicon (1.16 eV at 80 °K).[41]

The value of 0.58 eV from the optical-quenching spectrum is considerably smaller than the value of 0.69 eV reported by Loebner *et al.*[17] In the course of our investigation we also have observed higher apparent low-energy thresholds for quenching than the values reported here. The high apparent values result from high-quenching intensities, probably because both quenching and excitation result from the absorption of quenching-wavelength photons. Since $N_{\mathrm{Zn}^{-1}} \ll N_{\mathrm{Zn}^{-2}}$ under conditions used for optical quenching, quenching saturates at lower intensities than does excitation.

The observed temperature dependence of the Fermi level, i.e., $E_F = (0.51 - 3.5\times10^{-4}T)$ eV, has the following implications. The charge neutrality relation suitable for a system such as that shown in Fig. 9 is

$$N_{\mathrm{P}^+} + p \pm N_{X^\pm} = 2N_{\mathrm{Zn}^{-2}} + N_{\mathrm{Zn}^{-1}} + n, \qquad (3)$$

where N_{P^+}, $N_{\mathrm{Zn}^{-1}}$, and $N_{\mathrm{Zn}^{-2}}$ are the densities of ionized phosphorus, and singly and doubly ionized zinc, respectively. $N_{X^\pm}$ is the density of the unidentified center, the ± corresponding to the X imperfection being a single donor or a single accep-

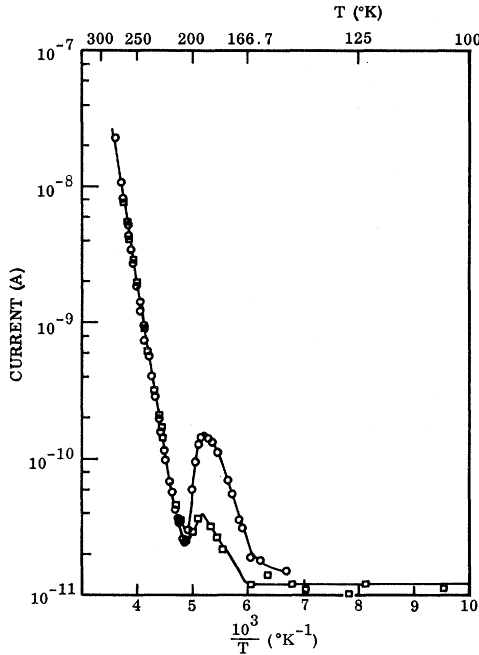

FIG. 8. Thermally stimulated current as a function of temperature after irradiation by (○) 0.9-μm light and (□) 2.0-μm light.

tor, respectively. For a Fermi-level location such as that in the present sample and over the temperature range of interest, $N_{P+} = N_P$ and n and p may be neglected in Eq. (3). Equation (3) may then be solved for the Fermi level with and without the term for the X imperfection. Without $N_{X\pm}$ Eq. (3) may be put in the form

$$E_F = E_2^c - kT \ln\left(\frac{N_P - N_{Zn}}{2N_{Zn} - N_P}\right) , \qquad (4)$$

where $N_{Zn} = N_{Zn^{-2}} + N_{Zn^{-1}}$. Equation (4) is consistent with the observed variation of E_F for $E_F(T=0) = 0.51$ eV $= E_2^c$, and $N_{Zn} = 0.503\ N_P$.

By contrast, if N_X is included in Eq. (3) as a donor, it is found approximately that $E_F(T=0)$ would be given by E_X^c (0.41 eV) and at higher temperatures $E_F < E_X^c$. Both characteristics are contrary to observation. If N_X is a single donor, Eq. (3) reduces to

$$E_F = E_X^c - kT \ln [N_x/(2N_{Zn} - N_P)]. \qquad (5)$$

If the X center is presumed to be a single acceptor the magnitudes of three terms in Eq. (3) are comparable and all depend on the Fermi energy so that a graphical solution is necessary. E_F is, under these circumstances, predicted to be about 0.454 eV at 200 °K and 0.458 eV at 300 °K. Evidently, the best fit between theory and observation occurs through excluding the X center from the charge-neutrality equation, for reasons not presently clear.

Density of Zn Centers

If the validity of Eq. (4) is assumed as a description of the thermal-equilibrium situation, it is seen that $N_{Zn} = 0.503\ N_P$, or if $N_P = 2\times10^{15}$ cm^{-3}, $N_{Zn} = 1.006\times10^{15}$ cm^{-3}.

In a trap-free material, it would be expected that the saturation value of the electron density for high intensities at low temperatures would be equal to N_{Zn}. However, the observed saturation density is 3×10^{14} cm^{-3}, somewhat smaller than the above value for N_{Zn}. Since photoexcitation at temperatures below about 180 °K results in filling the X traps with electrons, it is expected that

$$\Delta n_{sat} = N_{Zn} - N_X \quad . \qquad (6)$$

From the observed saturation value at 80 °K, $N_X = 7\times10^{14}$ cm^{-3} if the X traps are completely filled. This value is in good agreement with the value of $N_X = 10^{15}$ cm^{-3} estimated from the thermally stimulated conductivity data.

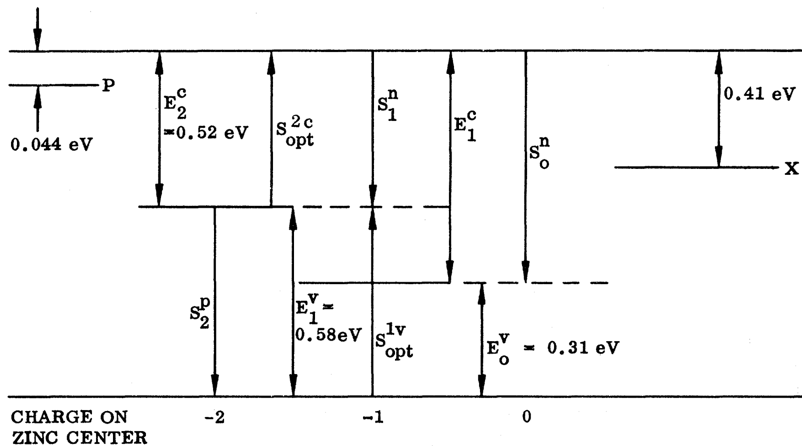

FIG. 9. Energy locations of the three defects found in the sample studied here. The densities are $N_P = 2\times10^{15}$ cm^{-3}, $N_{Zn} = 10^{15}$ cm^{-3}, and $N_X = 7\times10^{14}$ cm^{-3}. Solid lines indicate levels occupied by electrons, while dashed lines indicate levels occupied by holes. Note that the notation refers to the charge state of the center.

Scattering Cross Section of Zn Centers

The change in the value of $(1/\mu)$ is directly proportional to the change in cross section produced by photoexcitation. The experimental value for $\Delta(1/\mu)$ is 9×10^{-5} V sec/cm^2 for photoexcitation at 80 °K. Using $N_{\text{Zn}} = 10^{15}$ cm^{-3}, $\epsilon = 12$, and $m_e^*/m = 0.26$, the Brooks-Herring relation for mobility predicts a value of $\Delta(1/\mu) = 10^{-4}$ V sec/cm^2 for a change in charge of the Zn center from -2 to -1. Such close agreement may be fortuitous since use of the Brooks-Herring expression for such low values of electron density is questionable.

Electron-Capture Cross Section of Zn^{-1} Centers

Under the assumption that recombination in the samples investigated is controlled by the Zn impurity, two possibilities occur: (a) the simpler situation where recombination is dominated by capture of free electrons by Zn^{-1} centers and the density of Zn^0 centers is negligible, and (b) the situation in which temperature and/or photoexcitation effects produce a density of Zn^0 centers sufficiently large that they cannot be neglected in considering recombination.

The general expression for electron lifetime may be obtained by summing the recombination rates through the two levels. Under steady-state illumination the net capture rate of electrons (or holes) is equal to the recombination rate:

$$U_2 = N_{\text{Zn}^{-1}}\, n\beta_1^n - N_{\text{Zn}^{-2}}\,\beta_1^n n'$$

$$= N_{\text{Zn}^0}\,\beta_1^n\left(n\frac{N_{\text{Zn}^{-1}}}{N_{\text{Zn}^0}} - n'\frac{N_{\text{Zn}^{-2}}}{N_{\text{Zn}^0}}\right), \qquad (7)$$

$$U_1 = N_{\text{Zn}^0}\,\beta_0^n\left(n - \frac{N_{\text{Zn}^{-1}}}{N_{\text{Zn}^0}}n''\right), \qquad (8)$$

where $\beta_1^n = \langle v_n^2\rangle^{1/2} S_1^n$, $n' = N_c e^{-E_2^c/kT}$, $n'' = N_c e^{-E_1^c/kT}$, and U_1 and U_2 are the recombination rates through the lower and upper levels, respectively. The continuity equations for the populations of the two levels are

$$0 = N_{\text{Zn}^{-1}}\, n\beta_1^n + N_{\text{Zn}^{-1}}\beta_2^p p' - N_{\text{Zn}^{-2}}\, p\beta_2^p - N_{\text{Zn}^{-2}}\,\beta_1^n n', \qquad (9)$$

$$0 = N_{\text{Zn}^0}\, n\beta_0^n + N_{\text{Zn}^0}\, p''\,\beta_1^p - N_{\text{Zn}^{-1}}\, p\beta_1^p - N_{\text{Zn}^{-1}}\, n''\,\beta_0^n, \qquad (10)$$

where $p' = N_v e^{E_1^v/kT}$ and $p'' = N_v e^{E_0^v/kT}$. They may be solved for $N_{\text{Zn}^{-1}}/N_{\text{Zn}^0}$ and $N_{\text{Zn}^{-2}}/N_{\text{Zn}^0}$ for substitution in Eqs. (7) and (8).

Solving $N_{\text{Zn}} = N_{\text{Zn}^0} + N_{\text{Zn}^{-1}} + N_{\text{Zn}^{-2}}$ for $N_{\text{Zn}^{-2}}$ and Eq. (10) for $N_{\text{Zn}^{-1}}$, then substituting both in Eq. (9), we obtain an expression for N_{Zn^0}. When the final expression for N_{Zn^0} is substituted in Eqs. (7) and (8), we have expressions for the recombination rates through the two levels where N_{Zn^0}, $N_{\text{Zn}^{-1}}$, and $N_{\text{Zn}^{-2}}$ have been eliminated. The majority-carrier lifetime determined by recombination through a two-level center is then found to be

$$\tau_n = \frac{\Delta n}{U_1 + U_2} = \frac{\Delta n}{N_{\text{Zn}}}\,\frac{[(n\beta_0^n + p''\beta_1^p)/(p\beta_1^p + n''\beta_0^n)][\beta_2^p(p+p') + \beta_1^n(n+n')] + \beta_2^p p + \beta_1^n n'}{(\beta_2^p p + \beta_1^n n')[\beta_0^n(n - n''A) + A\beta_1^n(n - n'B)]}, \qquad (11)$$

where

$$A = \frac{n\beta_0^n + p''\beta_1^p}{p\beta_1^p + n''\beta_0^n}, \qquad B = \frac{n\beta_1^n + p'\beta_2^p}{p\beta_2^p + n'\beta_1^n}.$$

Under the assumptions of low temperature and low photoexcitation, Eq. (11) reduces to the simple form $(N_{\text{Zn}}\beta_1^n)^{-1}$ while under extremely high-illumination and low-temperature conditions it predicts simple recombination through the lower level, $\tau_n = (N_{\text{Zn}}\beta_0^n)^{-1}$. Still at low temperature, between the low- and extremely-high-excitation cases, $\tau_n = (n/p)\times(N_{\text{Zn}}\beta_1^p)^{-1}$. If n is presumed constant in the saturation region and p proportional to intensity, τ_n is inversely proportional to intensity.

Sah and Schockley[42] have derived an expression for U_2/U_1 from equations similar to (7)–(10). Evaluating it for the capture cross sections encountered here, it is found that $U_2 \gg U_1$, i.e., low-intensity single-level recombination occurs, for $T < 200$ °K ($S_1^n < 10^{-19}$ cm^2) and photoexcitation intensities in the linear range of photoconductivity vs intensity.

Under the above conditions the single-level-photoconductivity model described by Blakemore[43] may be used. If his general expression is reduced for the case of our sample, the electron lifetime may be written in the following simple form:

$$\tau_n = \tau_{n0}\,\frac{\Delta n + N_{\text{Zn}}}{\Delta n + (2N_{\text{Zn}} - N_{\text{P}})}. \qquad (12)$$

The electron lifetime is therefore independent of temperature except for the temperature dependence of the cross section S_1^n. The experimental measurements of τ_n from steady-state photoconductivity and decay of photoconductivity, plotted in Fig. 7, are expected to show the same temperature dependence as τ_{n0}, calculated from the measured value of S_1^n, and also plotted in Fig. 7. This is closely the case.

For direct comparison with τ_n, the values of τ_{n0} in Fig. 7 should be multiplied by 1.4 to account for the fact that 7×10^{14} cm^{-3} of the Zn centers are empty. Under thermal-equilibrium conditions,

$(2N_{Zn} - N_P) = 1.2\times10^{13}\text{-cm}^{-3}$ zinc centers would be expected to be unoccupied by electrons. However, under low-temperature, steady-state photoexcitation, all the electron traps (7×10^{14} cm^{-3}) must be filled leaving a corresponding number of zinc centers singly charged. Any further discrepancy between the curves, which cannot be considered experimental error, can be attributed to a slight error in the value of S^{1v}_{opt} used to calculate S^n_1 from the quenching data.

The data given in Table I and Fig. 5 indicate that the electron-capture cross section of the Zn^{-1} centers is approximately temperature independent below 80 °K and increases with an activation energy of 40 meV for temperatures between 100 and 200 °K. Each characteristic has been observed previously, but not both in the same material. Johnson and Levinstein[44] report an activation energy of 18 meV for the cross section of Au in Ge, whereas Williams[45] reports an energy of 10 meV for the same quantity. The capture cross section for Cu in Ge[46] is reported to vary as $T^{-1/3}$. Nearly-temperature-independent values for very small electron-capture cross sections associated with sensitizing centers in CdS, CdS-CdSe, GaAs, and InP have been reported by Bube and Cardon[39]; it was proposed that the lack of temperature dependence resulted from the absence of a repulsive barrier, the small cross section being associated with radiative recombination at a neutral center.

If we choose to write for the temperature-activated region,

$$S^n_1 = S^n_0\, e^{-E^*/kT}, \tag{13}$$

in which E^* represents the height of a repulsive barrier surrounding the neutral center, setting $E^* = 40$ meV gives $S^n_0 = 10^{-18}$ cm^2 in order for $S^n_1 = 10^{-19}$ cm^2 as measured at 200 °K. Such a value is much smaller than the value cited in Table I, and is much smaller than the cross section that would normally be expected for a neutral center. Also the value of $E^* = 40$ meV is much smaller than the height of the barrier expected from simple electrostatic arguments. On the other hand we may choose to write

$$S^n_1 = S^n_0\, W e^{-E^*/kT}, \tag{14}$$

where S^n_0 is the cross section for a neutral center and W is the tunneling transmission probability through a repulsive barrier at an average energy E^* above the conduction-band edge. Using S^n_0 from Table I and the measured values of S^n_1 and E^* at 200 °K, we obtain $W \sim 10^{-4}$. On the basis of our present knowledge it is therefore reasonable to associate the measured activation energy with that required for thermally assisted tunneling through a repulsive barrier about the singly negative zinc center,[47] and to associate the much smaller activation energy at low temperatures with essentially direct tunneling through the barrier.

CONCLUSIONS

Zinc impurity in high-resistivity n-type silicon has photoelectronic properties like those of sensitizing centers in II-VI and III-V compounds. The electron lifetime in our sample was increased by a factor of 10^4 to 10^{-1} sec at 80 °K by the incorporation of zinc impurity, and the sensitized photoconductivity could be optically quenched.

The energy level associated with the doubly negative zinc center was located 0.51 eV below the conduction-band edge, and 0.58 eV above the valence-band edge.

An increase in mobility is observed upon photoexcitation at low temperatures, which corresponds to a decrease in the charge of the zinc center from −2 to −1. The measured increase agrees quantitatively well with that predicted by the Brooks-Herring theory.

Models for recombination including either only electron capture by singly negative zinc centers, or electron capture by both singly negative and neutral zinc centers, were considered. For the conditions of our sample and experiment, a variation of electron lifetime with temperature was predicted to result only from a temperature dependence of the electron-capture cross section by singly negative zinc centers. This expectation was confirmed by finding the same temperature dependence for the electron lifetime measured from steady-state photoconductivity and from photoconductivity decay as that calculated from the independently measured capture cross sections. Quantitative agreement between these lifetimes was possible provided that the occupancy of zinc centers at low temperatures as affected by electrons held in traps was considered.

The electron-capture cross section of singly negative zinc centers was found to be about 10^{-20} cm^2 and temperature independent at temperatures below 100 °K, and to increase with an activation energy of 40 meV for temperatures between 100 and 200 °K. Thermally assisted tunneling through a repulsive barrier appears to be a reasonable interpretation of these results.

---

†From a thesis submitted by A. F. Sklensky in partial fulfillment of the requirements for the degree of Doctor of Philosophy at Stanford University.

*Supported by Lockheed Independent Research Funds.

[1]A. Rose, *Concepts in Photoconductivity and Allied Problems* (Interscience, New York, 1963), p. 43.

[2]R. H. Bube, *Photoconductivity of Solids* (Wiley, New York, 1960), p. 171.

[3]R. H. Bube, in *II-VI Compounds*, edited by J. S. Prener and M. Aven (North-Holland, Amsterdam, 1966), Chap. 13.
[4]R. H. Bube and L. A. Barten, RCA Rev. 20, 564 (1959).
[5]P. H. Kasai and Y. Otomo, Phys. Rev. Letters 7, 17 (1961); J. Chem. Phys. 37, 1263 (1962).
[6]J. Schneider, W. C. Holten, T. L. Estle, and A. Rauber, Phys. Letters 5, 312 (1963).
[7]R. Newman, H. Woodbury, and W. W. Tyler, Phys. Rev. 102, 613 (1956).
[8]R. Newman and W. W. Tyler, Phys. Rev. 96, 882 (1954).
[9]W. W. Tyler, R. Newman, and H. H. Woodbury, Phys. Rev. 97, 669 (1955).
[10]W. W. Tyler, R. Newman, and H. H. Woodbury, Phys. Rev. 98, 461 (1955).
[11]C. M. Penchina, *et al.*, Phys. Rev. 143, 634 (1966).
[12]E. Schibli and A. G. Milnes, Mater. Sci. Eng. 2, 229 (1967/68).
[13]Y. E. Pokrovsky and K. I. Svistunova, Fiz. Tverd. Tela 7, 1837 (1965) [Sov. Phys. Solid State 7, 1478 (1965)].
[14]J. L. Wagener and A. G. Milnes, Solid State Electron. 8, 495 (1965).
[15]H. Prier, J. Appl. Phys. 39, 194 (1968).
[16]J. S. Blakemore and C. E. Sarver, Phys. Rev. 173, 767 (1968).
[17]E. Loebner, U. S. Army Engineer Research and Development Laboratory Final Report No. H-P, Fort Belvoir, Virginia, 1966 (unpublished); E. E. Loebner and T. J. Diesel, Trans. AIME 239, (1967). N. R. Mantena and E. E. Loebner, in *Proceedings of the Third International Conference on Photoconductivity*, edited by E. M. Pell (Pergamon, New York, 1969), p. 53.
[18]B. V. Kornilov and A. V. Anfimov, Sov. Phys. Semicond. 1, 279 (1967).
[19]B. V. Kornilov, Fiz. Tverd. Tela 7, 1795 (1965) [Sov. Phys. Solid State 7, 1446 (1965)].
[20]B. V. Kornilov and S. E. Gorskii, Sov. Phys. Semicond. 2, 216 (1968).
[21]K. D. Glinchuk and N. M. Litovchenko, Fiz. Tverd. Tela 8, 2510 (1966) [Sov. Phys. Solid State 8, 2011 (1967)].
[22]C. S. Fuller and F. J. Morin, Phys. Rev. 105, 379 (1957).
[23]M. K. Bakhadyrkhonov *et al.*, Sov. Phys. Semicond. 4, 739 (1970).
[24]R. Sh. Malkovich and N. A. Alimbarashviti, Fiz. Tverd. Tela 4, 2355 (1963) [Sov. Phys. Solid State 4, 1725 (1963)].
[25]S. M. Zalar, J. Appl. Phys. 41, 3458 (1965).
[26]R. O. Carlson, Phys. Rev. 108, 1390 (1957).
[27]Yu. I. Zavadskii and B. V. Kornilov, Sov. Phys. Semicond. 1, 1103 (1967).
[28]B. V. Kornilov, Sov. Phys. Semicond. 2, 1480 (1969).
[29]K. D. Glinchuk, A. D. Denisova, and N. M. Litovchenko, Fiz. Tverd. Tela 5, 1933 (1963) [Sov. Phys. Solid State 5, 1412 (1964)].
[30]B. V. Kornilov, Fiz. Tverd. Tela 8, 201 (1966)[Sov. Phys. Solid State 8, 157 (1966)].
[31]B. V. Kornilov, Fiz. Tverd. Tela 7, 3458 (1965) [Sov. Phys. Solid State 7, 2794 (1966)].
[32]K. D. Glinchuk and N. M. Litovchenko, Fiz. Tverd. Tela 5, 3003 (1968) [Sov. Phys. Solid State 5, 2197 (1964)].
[33]B. V. Kornilov, Fiz. Tverd. Tela 6, 3721 (1964) [Sov. Phys. Solid State 6, 2982 (1965)].
[34]B. V. Kornilov, Fiz. Tverd. Tela 5, 3305 (1963) [Sov. Phys. Solid State 5, 2420 (1964)].
[35]Yu. I. Zavadskii and B. V. Kornilov, Phys. Status Solidi 42, 617 (1970).
[36]Yu. I. Zavadskii and B. V. Kornilov, Sov. Phys. Semicond. 5, 56 (1971).
[37]$1/Re$ is negligibly different from n.
[38]R. H. Bube and C. T. Ho, J. Appl. Phys. 37, 4132 (1966).
[39]R. H. Bube and F. Cardon, J. Appl. Phys. 35, 2712 (1964).
[40]T. S. Diesel, E. E. Loebner, and R. H. Bube, Bull. Am. Phys. Soc. 10, 1199 (1965).
[41]S. M. Sze, *Physics of Semiconductor Devices* (Wiley-Interscience, New York, 1969), p. 24.
[42]C. T. Sah and W. Shockley, Phys. Rev. 109, 1103 (1958).
[43]J. S. Blakemore, *Semiconductor Statistics* (Pergamon, New York, 1962), p. 280.
[44]L. Johnson and H. Levinstein, Phys. Rev. 117, 1191 (1960).
[45]R. L. Williams, J. Phys. Chem. Solids 22, 261 (1961).
[46]V. G. Alekseeva *et al.*, Sov. Phys. Semicond. 3, 1179 (1970).
[47]S. M. Ryvkin, I. M. Fishman, and Yu. G. Shreter, Sov. Phys. Semicond. 5, 1062 (1971).